Mineral precipitation in anammox granular sludge affects process performance, granules' morphology and microbial community

C. Polizzi[1*], T. Lotti[1], A. Ricoveri[2], R. Campo[1], C. Vannini[2], M. Ramazzotti[3], D. Gabriel[4], G. Munz[1]

[1] Department of Civil and Environmental Engineering, University of Florence, Via di S. Marta, 3, 50139, Firenze, Italy

[2]Department of Biology University of Pisa Via A. Volta 4, 56126, Pisa Italy

[3]Department of Biomedical, Experimental and Clinical Sciences "Mario Serio" University of Florence, Viale Morgagni 50, 50134, Firenze, Italy

[4] GENOCOV Research group, Department of Chemical, Biological and Environmental Engineering, Escola d'Enginyeria, Universitat Autònoma de Barcelona, 08193 Bellaterra, Spain

* Corresponding author: cecilia.polizzi@unifi.it; Via di S. Marta 3, 50139, Firenze, Italy

Abstract

When treating wastewaters prone to inert precipitation with granular sludge systems, mineral formation needs to be properly controlled to ensure system's long-term stability. In this work, an extensive study on mineral precipitation on the surface of anammox granular sludge is presented. A 7-L reactor was inoculated with one-year stored biomass and volumetric load up to 0.48 gN-NO_2^-/l/d were achieved, with nitrite removal above 95%. Severe mineral precipitation was observed on the granules' surface, after two months of hard-water feeding and resulted in a dramatic deterioration of reactor performance. Substrate diffusion limitation in the inner layers, insufficient mixing due to higher granule density and shear stress increase were deemed the main mechanisms that lead to progressive process disruption. Gravimetric selection was applied to discard granules affected by precipitation and allowed for process restoration.

Mineral composition as well as its impact on reactor performance, biomass activity and microbial population were investigated.

Keywords: Anammox, granular sludge, mineral precipitation, long-term stability

1. Introduction

Anaerobic ammonium oxidation (anammox, AMX) remains at the forefront of the innovative biological treatments for nitrogen removal, due to the significant contribution towards energy autarchy and resource optimization in wastewater treatment facilities. Its application to side-streams and to some industrial wastewater is considered an established technology and current implementations rely on the synergy of partial nitritation and anammox (PN/A) processes, allowing for a complete autotrophic nitrogen removal and a significant reduction in oxygen requirement compared to conventional treatments (nitrification/heterotrophic denitrification). Further advantages can be achieved if granular sludge technology is adopted: (i) effective retention of the slow-growing biomass; (ii) superior sludge settleability properties; (iii) optimization of the microbial community composition. Nevertheless, AMX full-scale implementation worldwide is still limited (Xue et al., 2021), despite the astonishing attention that the research field has devoted to the novel process in the last decades. Among the obstacles hindering the widespread application of the AMX process there is the long start-up time required by the slow-growing biomass (Ali et al., 2014). Seeding with a selected inoculum is a successful solution to achieve rapid start-up or reactor rescue in case of unexpected failures and long-term biomass storage is a key issue to ensure biomass availability when needed (Ali et al., 2014).

Moreover, the composition of real wastewater can impact the long-term stability of granular AMX systems, either due to unbalanced nutrients and/or ions concentrations or for the presence of potential inhibitory compounds. When AMX granular technology is applied to streams prone to mineral precipitation, such as anaerobic digestion supernatant, landfill leachate or in wastewater reuse systems, the implications of mineral formation on process performance and stability should be carefully assessed and controlled (Langerak et al., 1997; Wu et al., 2018). Mineral precipitation has been reported to occur in granular biomass systems, either in anaerobic digestion (AD), partial-nitritation/anammox (PN/A), anammox (AMX) and aerobic granular sludge (AGS), both in lab-scale as well as in real-scale applications (Langerak et al., 1997; Lin et al., 2013; Ma et al., 2020). Precipitate formation strongly depends on influent composition and operational/process conditions such as pH and process influence on pH. Yet, two types of minerals are mainly reported: carbonated minerals and phosphate-bonded minerals; the presence of metal ions, such as calcium and magnesium, is also crucial. Ad-hoc pre-treatment or operation strategies are recommended when dealing with wastewaters rich in Ca or Mg: (i) mineral precipitation can be enhanced in a preliminary unit to prevent scaling drawback in the subsequent reactor or (ii) the formation of inert-rich granules can be promoted within the same biological reactor coupled with the withdrawing of the high-density biomass from reactor's bottom (gravimetric selection). The latter option is feasible in case of biologically-induced mineralization (Johansson et al., 2017). As a matter of fact, enhanced Ca-P mineral precipitations in granular biomass has received growing attention for simultaneous N removal and P recovery in anammox granular sludge (Guo and Li, 2020; Ma et al., 2020).

According to other works reported in the literature, the positive or negative impact of mineral precipitation on granular biomass is function of the extent of the inert formation, as well as its composition and location (Langerak et al., 2000; Lin et al., 2013). From the one hand, mineral precipitation allows for better settleability, higher density and improved mechanical strength of granules (Lin et al., 2013). Also, the common phenomenon of granule floatation, and consequent biomass washout, is reported to be effectively reduced in case of controlled P-precipitate formation in the AMX granules (Xue et al., 2020). From the other hand, excessive inert concentration would be detrimental due to possible substrate diffusion limitation, reduction of active biomass sites and, ultimately, to granule or granular bed complete mineralization (Langerak et al., 2000). Indeed, uncontrolled inert accumulation in granular sludge and consequent loss of biomass activity are important factors often overlooked in real plants.

In the present work, a gas lift reactor was inoculated with PN/A granular biomass after more than one-year storage and synthetic influent rich in Ca and inorganic carbon was fed during 3 out of 9 months of operation. The first objective of the present work was to challenge fast reactor start-up with the long-term stored biomass. Then, the issue of mineral precipitation was addressed with the objective of investigating the mechanisms that lead to a severe mineral formation and evaluating the effect on granules morphology, biomass activity and microbial composition. To the best of our knowledge, this is the first study evaluating the long-term impact of surface mineral precipitation on anammox granular reactors.

2. Materials and methods

2.1 Gas-lift reactor

A 7-liter up-flow gas-lift reactor was run for more than 270 days. Figure 1 presents a schematic of the reactor. Internal gas recirculation was accomplished by a vacuum pump providing a flowrate of around 1 l/min. Reactor headspace was maintained at a slight overpressure of 0.05 bar, visually checked by a pressure-control water lock. A mixture of N_2 and CO_2 (95% and 5%, respectively) was provided manually every day (except weekends), at a flowrate of 0.1 l/min for 20 minutes. Influent was provided by a peristaltic pump. A U-shape tube was placed prior to the effluent collection tank and acted as a settling control unit. Temperature, pH and ORP were monitored by two probes (5336T Hach Lange for pH and T; 5361 Hach Lange for ORP). Apart from exceptional events, pH was around 8.1-8.4 and no pH control was implemented. Temperature was maintained at 30±2 °C, by mean of continuous tempered water recirculation in reactor's jacket. HRT was maintained at 1.1 d for the first 40 d period, and then increased to 1.6 d from day 41 on. The experimental set-up and the consequent laboratory activities were carried out in the laboratory facilities of the tannery wastewater treatment plant, WWTP (Consorzio Cuoiodepur S.p.a., Pisa, Italy).

Figure 1 Experimental set-up. Water line (blue), gas line (dashed red) and sensors (dotted green). Influent port (1); gas recirculation inlet (2); water-lock and overpressure control (3); moisture trap (4); vacuum pump (5); thermostatic unit (6).

Nitrite and Ammonium concentrations in the synthetic influent (Graaf et al., 1996) were set according to the experimental phases and added as $NaNO_2$ and NH_4HCO_3 or $(NH_4)_2SO_4$. Distilled water was used for the preparation of the mineral medium, except for the period from day 55 to 135, during which tap water was used instead (well water used in Cuoiodepur WWTP for process operations). The concentration of the main alkalinity-related components in the tap water is presented in table 1. The estimated values corresponding to the mineral medium prepared with distilled water (days 36-50 as reference period) and tap water (days 60-120) are also reported in the same table.

Table 1 Tap water and mineral medium characterization for alkalinity, total phosphorous and hardness related components.

The reactor was inoculated with 500 ml of settled granular biomass from the PN/A plant in Olburgen WWTP, the Netherlands (Abma et al., 2010). Initial volatile suspended solid (VSS) concentration in the reactor was about 2.5 gVSS/l. Prior to seeding, the inoculum biomass was kept at 4°C for 13 months, ensuring a minimum bulk concentration of 100 mgN-NO_3^-/l, with check on pH and conductivity every 10 days. Regular mixing was provided manually and supernatant was partially renewed with fresh water or nutrient-free mineral medium, when pH and conductivity showed increase higher than 0.5 and 0.5 mS/cm, respectively.

Nitrogen species (ammonium, nitrite and nitrate) were monitored daily, except during weekends. Total and volatile suspended solids (TSS and VSS) were characterized every other week by withdrawing samples from the mixed zone. Also, concomitant TSS and VSS characterization of solids retained in the U-shaped effluent tube was performed. Solids retained in the U-tube were removed from the system, apart from specific cases of intense granule flotation and washout, during which granules were re-introduced in the system. No other active SRT control was performed and SRT resulted in the range 200-300 d.

2.2 Experimental phases

Four experimental phases are presented and described in table 2. Throughout the experiment, influent ammonium/nitrite ratio was maintained at least at the stoichiometric value and, more frequently, slightly above operating under nitrite-limiting conditions. Phase 1 (P1, days 1-15) aimed at biomass reactivation and reactor start-up; ammonium and nitrite inlet concentration were 100 to 200 mgN-NH_4^+/l and 45 to 200 mgN-NO_2^-/l, respectively, with a weekly stepwise increase of 50 mgN/l for nitrite. An inlet concentration of 150 mgN-NO_3^-/l was dosed as redox buffer. Also, 10 mgCOD/l as acetate were added to restore glycogen storage that might have been consumed due to one-year starvation (Niftrik et al., 2008). The aim of Phase 2 (P2, days 16-130) was to maximise the reactor removal capacity by progressively increase inlet concentration, i.e. inlet load. In a few cases, nitrite accumulation raised up to 100 mgN-NO_2^-/l. At the occurrence of these events, the feeding was paused and the reactor was operated in batch condition until nitrite concentration decreased to less than 40 mgN-NO_2^-/l. Phase 3, (P3, days 131-154), was characterized by intense mineral precipitation on the granules' surface and concomitant process instability and deterioration. Severe increase of nitrite concentration and a change in granules appearance was observed together with. An off-site rescue procedure was implemented during days 155-177 as described in section 3.1 (not reported in process performance graphs). Process stability was restored in phase 4 (P4, days 178-270) at a NLR of 0.22 gN-NO_2^- /l/d.

Table 2 Applied conditions during the experimental phases.

As ammonium was intentionally dosed in excess (nitrite-limiting conditions), Nitrogen Loading Rate (NLR), Nitrogen Removal Rate (NRR) and Specific Nitrogen Loading Rate (SNLR) were referred to the sole nitrogen-nitrite. The SNLR was calculated as the applied NLR specific for the VSS content of the reactor. General stoichiometry was checked by means of mass balances on the nitrogen compounds.

2.3 Activity batch tests

Two types of activity batch tests were performed: in-situ tests and manometric tests. In-situ tests were conducted by operating the reactor in batch-mode. In case of nitrite accumulation (above 80 mgN-NO_2^-/l), the inlet was stopped, the reactor was operated in batch-mode and samples were collected every 45 or 120 minutes to assess the maximum removal capacity of the reactor (NRR_{max}, gN/l/d). Manometric tests were conducted in 300-ml Oxitop® bottles, similarly to the procedure adopted by Lotti et al. (2012). Fresh biomass was withdrawn from the mixed zone of the reactor and re-suspended in nutrient-free mineral medium. A mixture of N_2/CO_2 (95%,5%) was sparged in the headspace to ensure anoxic conditions. Bottles were placed in a pre-heated incubator at 30°C. Continuous mixing was provided by an orbital shaker set at 180 rpm.
Concentrated pulses of 1 M $(NH_4)_2SO_4$ and 1M $NaNO_2$ solutions were spiked in order to provide 30 to 80 mgN/l, as nitrite and ammonium, in the liquid phase. A minimum NH_4^+/ NO_2^- ratio of 1 was ensured. When N_2 exponential production phase was followed by stable pressure plateau, a further pulse of concentrated solutions was provided. In each test, a minimum of three and a maximum of five consecutive spikes were provided in order to have a more robust estimation of the maximum activity. After

each test, the total amount of biomass was used for VSS assessment. On average, biomass concentration ranged from 0.6 to 1.2 gVSS/l.

Manometric tests allowed to assess the maximum specific anammox activity (MSAA), expressed as gN/gVSS/d, whereas the in-situ batch tests allowed the estimation of the maximum removal capacity of the reactor (NRR_{max}, gN/l/d). These two data were matched with the reactor VSS concentration in order to be straightforwardly comparable. A total of 10 activity tests were performed. As above, due to the applied nitrite-limiting condition, MSAA and SNLR were referred to the sole nitrogen-nitrite (Dapena-mora et al., 2004).

2.4 Analytical methods

Ammonium, nitrite and nitrate were measured spectrophotometrically, using commercial kits (Dr Hach Lange). VSS and TSS were assessed according to standard methods (APHA, 2005). The following parameters were analysed on tap water: (i) Ca, K, Mg, Na by ionic chromatography (UNI EN ISO 14911:200, from an external laboratory); (ii) total alkalinity according to Italian standard regulations (method 2010 B APAT and IRSA CNR, 2003, from an external laboratory) and metals and total phosphorous by Inductively Coupled Plasma Optical Emission Spectrometry, ICP-OES (Optima 2100 DV ICP-OES, PerkinElmer). Acid tests were performed on the inert formation by applying a few drops of 1M HCl in order to assess the presence of carbonate-related minerals. Also, qualitative assessment of total and carbonate-related alkalinity was obtained through commercial Quantofix® test strips.

2.5 Microbial community study, granular size distribution and analyses with electron microscopy

Biomass samples were collected every 30-45 days for Next Generation Sequencing (NGS) analyses. Primers couple from Takahashi et al. (2014), with a slightly modified forward primer, optimised for anammox bacteria were used for PCR amplification of the V3 and V4 variable regions of the 16s rRNA gene (Mazzoli et al., 2020). Amplicons were then sent to an external laboratory (BMR Genomics, Padua, Italy) for high throughput sequencing through Illumina MiSeq, achieving 2x300 bp sequencing. Bioinformatics elaboration was performed according to Niccolai et al. (2020). Granular size analyses were performed by mean of image elaboration through the software Image ProPlus® (Tijhuis and Loosdrecht, 1994). SEM-EDX and TEM analyses were performed on a dozen of granules in order to study their superficial appearance and composition as well as the internal structure. For SEM-EDX samples preparation, an overnight fixation with 2.5% glutaraldehyde and 0,1 M BPS was conducted; then, repeated rinsing with the same BPS were performed prior to dehydration at increasing ethanol concentrations (50% to 100%) and, subsequently, at hexamethyldisilazane (HMDS). Dried samples were coated with Gold and Platinum, prior to their analysis. For TEM sample preparation, fixation was performed in glutaraldehyde and osmium tetroxide according to the procedure by Lin and Wang (2017); samples were then embedded in Epon-araldite resin, sectioned with an RMC PowerTome X ultra-microtome and stained with uranyl acetate and lead citrate. TEM observations were conducted with a JEOL JEM-100SX electron microscope.

3. Results and discussion

3.1 Reactor operation

Reactivation phase P1 was relatively fast as noticeable nitrite and ammonium removal was observed after the first two weeks of operation (figure 2a). Nitrite effluent concentration stayed below 10 mgN-NO_2^-/l, and a proportional nitrate increase was shown as well, indicating active growth of anammox bacteria (Lotti et al., 2014). Since the concept of *reactivation* is not absolute, in the present work, reactivation refers to the positive response of the biomass to the applied nutrient load, i.e. no nutrients were accumulated in the effluent. During P2, the relatively high pace in influent nitrogen concentration (75% NLR increase in less than 10 days) lead to nitrite accumulation up to 80 mgN-NO_2^-/l, on day 37. On this day, inflow was paused, and an in-situ activity tests performed (see section 3.2). Results showed that the applied NLR was above the NRR_{max} of the system (0.30 vs 0.23 mgN-NO_2^-/l/d, applied NLR vs NRR_{max}, respectively). Moreover, granules flotation was observed in those days and biomass washout was likely contributing to process instability. Granules floatation has been reported by many authors (Chen et al., 2014; Dapena-mora et al., 2004; Li et al., 2014) as related to system overloading and consequent nutrient accumulation in the bulk as some of the major causes. Indeed, granules floatation was observed when bulk NO_2^- concentration was around 80-100 mgN/l. Consequently, NLR was lowered by decreasing the flowrate from 7 to 4 l/d. The resulting 1.6-day HRT was kept from this day on. From day 35 to 70 stable operation was maintained to avoid overload conditions. After this period, nitrite removal efficiency was constantly higher than 95% (fig. 2b) and the biomass appeared with a bright carmine colour, smaller in size and with a more uniform granular dimension (see section 3.3). NLR increase strategy was started again on day 71. Yet, since day 90 to day 120, a slight but progressive process disruption was observed together with an increase in pH and decrease in VSS/TSS ratio, witnessing the intense mineral precipitation affecting the granules in that phase. Regular episodes of nitrite (and ammonium) accumulation occurred and resulted in concentrations up to 80 and 102 mgNNO_2^-/l on day 103 and 117, respectively (fig. 2a). Nitrite accumulation showed chronical after day 130, despite contingent measures as the reduction of influent nitrite concentration (days 120-130).

Figure 2 Influent and effluent nitrogen concentration (a); NLR and NO_2^- removal efficiency (b). Nitrate was dosed in phase 1 only, at influent concentration of 150 mgN-NO_3^-/l.

As shown in figure 3, beside a gradual increase in the overall VSS concentration, a dramatic decrease in VSS/TSS ratio was observed from day 60 to day 140. On day 83, a VSS/TSS ratio decrease of around 30% was observed and the decrease in VSS/TSS remained almost linearly until day 140 when the lowest VSS/TSS ratio (35%) was registered. Concomitant changes in granule appearance and density were observed: granules progressively turned from bright red to whitish and their density increased notably, since usual agitation provided by gas flow recirculation was not sufficient to suspend the biomass, which started to settle at the bottom of the reactor. Further evidence, discussed in sections 3.4 and 3.5, showed that the increase in the non-volatile fraction of TSS (NVSS) was mainly due to a mineral deposition on the surface of the granules after two-month feeding with hard tap water (fig. 3). Acid tests on the granules' mineral ash indicated that the minerals had a high carbonate content as the characteristic fizzing was observed. Substrate diffusion limitation from the bulk to the inner layers was deemed mechanisms that lead to progressive process disruption.

Insufficient mixing due to higher granule density and shear stress increase due to hard-particle collision were also considered responsible as cascade effects.

Figure 3 VSS concentration in the reactor and VSS/TSS ratio. Dotted vertical lines define the hard-water feeding period.

On day 155, the reactor was emptied, and an off-site rescue strategy was implemented with the aim of removing granules severely affected by mineral precipitation. As a fact, precipitation did not affect all the granules at the same extent. Some appeared completely covered of a whitish shell whereas others appeared almost free from any deposition (fig. 6a). The rescue procedure was as follow: (i) gravimetric selection was applied exploiting the high density of mineral-covered granules; (ii) selected biomass was re-suspended in HEPES-buffered medium at pH 6.5 for five consecutive days, replacing the slightly acid medium every day, in order to dissolve residual carbonate minerals as much as possible.

The rescued biomass was almost half of the total biomass present in the reactor during the reference period of days 130-150 and was inoculated back in the reactor on day 178 and the restoring phase, P4, started. An in-situ activity test was performed in order to set the proper NLR according to the system capacity. In order to promote the residual carbonates dissolution, a Calcium-free synthetic medium was prepared, $NaHCO_3$ was dosed at 400 mg/l and influent pH was lowered to 6.5. Taking into account that the biomass was halved and underwent critical conditions, a 60% reduced NLR was applied. From day 200 on, stable NLR of 0.22 gN-NO_2^-/l/d was applied at HRT of 1.6 d, and a stable 95% nitrite removal efficiency was established.

Table 3 shows the observed stoichiometry throughout the experimental phases as gN-$NO^-_{2\_removed}$/gN-$NH_4^+{}_{\_removed}$ and gN-$NO_3^-{}_{\_produced}$/gN-$NH_4^+{}_{\_removed}$. Results were in agreement with the stoichiometry reported by Lotti et al. (2014). A slight increase in both N ratios were observed during the most critical periods (P3 and first days of P4). It can be speculated that an additional ammonium release could be derived from cellular lysis (ammonification) in the inner layers, thereby affecting the measured ratios.

Table 3 Observed stoichiometry during the operational phases

3.2 Activity tests

Manometric and in-situ batch tests showed comparable results when both types of tests were performed within a few days, corroborating the applied stoichiometry as well as the reliability of the methods (fig. 4). On day 36 and 47 the MSAA was 0.155±0.004 gN-NO_2^-/gVSS/d, considering results from both types of test, and it more than doubled after one month, reaching 0.349±0.034 gN-NO_2^-/gVSS/d, at day 83, confirming the successful biomass reactivation and the fast reactor start-up. The progressive process disruption observed in the reactor was reflected in a decline in MSAA on days 117 and 135, with a decrease of the 21% and 59%, respectively, compared to the maximum value observed on day 83. Successful process restoration after biomass rescue and segregation, was proven by subsequent increase of the MSAA on day 178 (after re-inoculation) up to its maximum value of 0.387±0.027 gN-NO_2^-/gVSS/d observed on day 218, maintained quite stable also on day 245. On days 35, 47 and 135 the SNLR was higher than the MSAA of the biomass; consistently, nitrite accumulation was observed in those days. In phase 4 (days 218 and 245), as the MSAA raised again to the highest values observed in day 83, the constant SNLR applied ranged 60-65% of reactor's maximum capacity.

Figure 4 Results on activity tests versus the applied SNLR. MSAA from manometric assays (black columns) and from in-situ batch tests (white column), as average and standard deviation values; SNLR (--o--).

3.3 Microbial community and granular size distribution

Size distribution analyses were performed on the inoculum biomass and on day 40 and 260, as well as on floating granules collected during severe floating events on days 40-50. After 40 days of operation, granules' average diameter (1.11 mm) was lower than the one of the inoculated sludge (1.55 mm). A higher average diameter of 1.82 mm was observed on day 260 (P4, after process restoration), when the diameter values falling in the 10^{th}, 50^{th} and 100^{th} percentile were much closer among each other in comparison with those of previous samples, witnessing higher homogeneity in granular size distribution. Floating granules exhibited by far the highest average diameter of ca 3 mm, in agreement with other works (Chen et al., 2010; Dapena-mora et al., 2004).
In figure 5, the microbial distribution in terms of relative abundance is presented at class (a) and genus level (b). *Planctomycetia* was the class showing the highest relative abundance in all the samples, whose percentage remained almost constant throughout the experimental phases, namely 38±3%. At genus level, anammox bacteria were related to "*Ca.* Brocadia" and "*Ca.* Kuenenia" and an interesting population change within them was observed. "*Ca.* Brocadia" was the predominant planctomycetes on days 49, 105 and 232 with relative abundance of 38%, 35% and 25%. Only the sample on day 190 showed a significantly lower relative abundance (15%) in "*Ca.* Brocadia". A complementary behaviour was observed for "*Ca.* Kuenenia" which was almost absent on day 49, but its relative abundance achieved 5% and 19% on day 105 and 190, respectively, and decreased to 8% on day 232. On day 49 (Phase 2), the reactor was

responding very well to the fast increase in NLR, whereas on day 190 process deterioration was evident due to the intense precipitation. "*Ca.* Brocadia" is reported to be a r-strategist organism and "*Ca.* Kuenenia" a k-strategist instead (Oshiki et al., 2016). Under the assumption that severe precipitation hindered substrate diffusion within the granule, substrate-limiting conditions might have resulted in the internal layers, where anammox used to thrive on high substrate concentrations, promoting a (temporary) advantage of "*Ca.* Kuenenia" over "*Ca.* Brocadia". In line with such an assumption, the evidence that "*Ca.* Brocadia" returned to be the predominant anammox genus as the process stability was restored and the most damaged biomass removed.

Figure 5 Microbial diversity profiles over the experimental work, at class (a) and genus level (b). Only Operational Taxonomic Units with relative abundance higher than 1% are displayed.

3.4 Mineral precipitation

Figure 6a shows the macroscopic appearance of the granules affected by severe mineral deposition and their inorganic shell after incineration at 550°C. Granules ash looked like whitish mineral shell around the granules.

As reported in tab. 1, the final concentration of Ca, Mg and inorganic carbon (as bicarbonate ion) was as high as 187, 55.4 and 495-730 mg/l, on days 60-120. The software Visual MINTEQ 3.1 (Gustafsson, 2014) was used to calculate the saturation index of each possible compound, according to the concentrations of tab. 1, pH and temperature conditions. Saturation Index is expressed as:

$$SI = log\frac{IAP}{K_{ps}}$$

where IAP is the Ionic Activity Product and K_{ps} is the solubility product of a given compound (Ma et al., 2020). SI values higher than 0 indicate super saturation conditions, i.e. the possibility of precipitation. The condition with the highest nitrogen load was considered (upper limits of C-HCO_3^- and Na^+ concentration ranges, tab. 1), as a worst-case scenario. Software prediction on mineral precipitation were: (i) calcite, around 2 mM; (ii) dolomite, around 2 mM and, in a little extent (iii) hydroxyapatite, around 10^{-2} mM. As already discussed, PO_4-bonded minerals, are reported as common precipitates in anammox granules. ICP-OS analysis carried out on tap water and effluent samples (on days 140 and 180), shows values of 0.07±0.01 and 3.77±1.1 mgP_{tot}/l, respectively. Since influent P- PO_4^3 was dosed at around 5 mg/l, the total P concentration in reactor effluent witnesses that the majority of P-PO_4^{3-} was exiting the system, net of biomass uptake and possible marginal precipitation, confirming the hypothesis that the visible mineral precipitate was not belonging to any of the Ca-PO_4 bonded minerals.

The location of mineral precipitation is also of interest. Most of previous works report precipitation as occurring in the core of the granule, and several reasons have been proposed to support this evidence. First, mineral precipitate nuclei can form in the bulk liquid and may act as supporting material for granule formation; then, the inner region of the granule is typically less active, with a higher pH and more abundant in inert cellular-lysis product and minerals, compared to the external layers. Undesired carbonates precipitation *into* AMX granules has been reported recently by Ma et al. (2020), during the operation of enhanced precipitation of hydroxyapatite in the bioreactor, at bulk pH of 8.5 or above. In the present study, carbonate precipitation occurred at lower pH, around 8.1; yet, the saturation pH, as defined by (Langelier, 1936), strongly depends on the level of calcium and bicarbonate, the latter being ca 8 times higher in the present work compared to Ma et al. (2020). Precipitation *onto* the surface of AMX granular biomass seems far more unusual and it has been experienced by Trigo et al. (2006) and Zhang et al. (2017), both operating AMX systems with synthetic influent and observing undesired apatite-like and calcite-like precipitation, respectively.

In this work, the evidence that the precipitation occurred on the surface of the granules and did not affect other surfaces on the bulk liquid (such as submersed probes or tubes) suggested that the precipitation reaction was somehow locally induced by biological processes (Johansson et al., 2017). Local pH gradients at the granule surface, due to the proton-consuming AMX activity, are likely to be the major drivers to promote local precipitation offering a favourable surface for incipient calcite precipitation and the consequent deposition. The calcium concentration observed in the present study is within the range of 40-600 mg/l reported to promote anaerobic sludge granulation (Chen et al., 2020) and even higher concentration can be found in landfill leachate and industrial wastewaters where lime is used as buffering agent (Langerak et al., 1997). Thereby, intense mineral formation is pointed as an important warning for real-scale treatment of such streams.

3.5 SEM-EDX and TEM analyses

SEM and EDX analysis showed that the general morphological appearance of the granules exhibited the typical cauliflower-like aspect with concavities and irregular pattern (Arrojo and Campos, 2006; Kang et al., 2019). Average O/C molar ratio was calculated over the spectrum analyses in 8 internal and three external points on a precipitate-free granule and resulted in a 0.56±0.19, slightly higher than the value of anammox biomass composition of $CH_{1.74}O_{0.31}N_{0.20}$ (Lotti et al., 2014), more in line with the O fraction in the general formulation of biomass $CH_{1.8}O_{0.5}N_{0.2}$ (Heijnen et al., 1992). Biomass composition by Lotti et al. (2014) was estimated from an almost pure culture of free-living anammox cells, a condition far different from the one in the present study, with granular sludge (EPS-rich VSS) with an almost complete sludge retention. Calcium fraction results in negligible concentration (below 5% in weight). In figure 6b, SEM images on granules with evident mineral precipitation allow to distinguish a thin uniform surface reminding to biofilm aggregates and a more irregular and rough surface reminding inorganic structures. EDX analyses revealed that Ca was much more abundant in the irregular surface, compared to the biofilm-like one. Phosphorus was not detected in any of the analysed areas, confirming that the inert precipitation was not related to phosphate-bond minerals. EDX analyses over several points and areas of the surfaces with precipitate-like appearance returned a Ca/C molar ratio ranging from 0.9 to 2.5, confirming that the mineral was $CaCO_3$-like as predicted by the saturation indexes (section 3.4). The higher values observed suggest either that others Ca-based minerals were present, or that the results on the analysed areas were affected by biofilm aggregates interference (not-clearly distinguishable). TEM analyses showed that granules not affected by precipitation (withdrawn in phase 4) showed a dense presence of the typically round shaped anammox, with the usual concavity on the cellular wall (fig. 6c). A tertiary organization in AMX granules' structure with a first level of aggregation among few cells (clusters or zoogloeae), a secondary aggregation embedded by EPS and a tertiary cementation of aggregates has been proposed by Lin et al. (2017) and Kang et al. (2019). Such a sub-unit structure is clearly represented for granules free from precipitation, where microorganisms other than AMX were detected in the interspaces among (and not within) bacteria agglomerates. A lower resolution was obtained in samples affected by significant precipitations, probably due to a lower efficiency in the preliminary fixation procedure, possibly related to limited diffusion of reactants due to the mineral shells. As a general consideration for precipitate-affected granules, AMX cells appear more dispersed and non-anammox microorganism are encountered more randomly over the analysed areas. Similar evidences were reported by Hu et al. (2018), comparing anammox granules grown under nutrient abundance (dense cell agglomeration) *vs* nutrient limitation (dispersed cell distribution). In the present work, it is, in fact, assumed that mineral precipitation lead to nutrient diffusion limitation along the granule section.

Figure 6 Pictures of anammox granular biomass on day 155: on a 0.5-mm sieve on the left and after incineration at 550° on the right (a). SEM images of a granules showing evident mineral precipitation exhibiting two types of surfaces: a biofilm-like uniform layer over a rough irregular surface with crystal precipitates (b). TEM observations on sections of granules not affected by mineral precipitation on the left and with evident precipitation on the right (c).

Conclusions

In the present work we demonstrate that a fast reactor start-up with long-term stored biomass is possible if proper storage of active AMX granules is provided. Besides, the study presents a comprehensive study on the problem of mineral precipitation in AMX granular sludge. Three months feeding with hard water resulted in a peculiar formation of mineral shell over the granules that impacted process performance, granular sludge morphology and microbial composition. Substrate diffusion limitation within the granule is deemed the main mechanism that led to biomass activity loss. Such a condition likely provided a temporary advantage of the k-strategist "*Ca.* Kuenenia" genus over the r-strategist "*Ca.* Brocadia", the last being the dominant during the rest of the experimental period. The integrated results from chemical analyses, simulated precipitation conditions and SEM-EDX analyses indicated that the inert formation was calcium and carbonate-based, likely to be formed in waters with high calcium and carbonate-related alkalinity. Gravimetric selection showed to be an effective solution for discarding granules with excessive precipitation and recover system performance, such a criterion can be applied also in real-scale applications. Careful monitoring of the VSS/TSS ratio as well as the regular withdrawal of the denser granules from reactor's bottom are suggested for inert accumulation control.

Supplementary data of this work can be found in online version of the paper.

Acknowledgement

The present work was supported by a financial contribution from Consorzio Cuoiodepur S.p.a. (Pisa, IT) and was partially developed within the H2020-MSCA-RISE-2019 Project Recycles (GA: 872053).

References

2. Abma, W.R., Driessen, W., Haarhuis, R., Loosdrecht, M.C.M. Van, 2010. Upgrading of sewage treatment plant by sustainable and cost-effective separate treatment of industrial wastewater. Water Sci. Technol. 61, 1715–1722. https://doi.org/10.2166/wst.2010.977
3. Ali, M., Oshiki, M., Okabe, S., 2014. Simple , rapid and effective preservation and reactivation of anaerobic ammonium oxidizing bacterium " Candidatus Brocadia sinica ." Water Res. 57, 215–222. https://doi.org/10.1016/j.watres.2014.03.036
4. APAT, IRSA CNR, 2003. IRSA-CNR Metodi analitici per le acque.
5. APHA, 2005. APHA: Standard methods for the examination of water and wastewater, 21st ed. ed, American Public Health Association/American Water Works Association/Water Environment Federation,. Washington DC.
6. Arrojo, B., Campos, J.L., 2006. Effects of mechanical stress on Anammox

granules in a sequencing batch reactor (SBR). J. Biotechnol. 123, 453–463. https://doi.org/10.1016/j.jbiotec.2005.12.023

7. Chen, H., Ma, C., Yang, G., Wang, H., Yu, Z., Jin, R., 2014. Floatation of flocculent and granular sludge in a high-loaded anammox reactor. Bioresour. Technol. 169, 409–415. https://doi.org/10.1016/j.biortech.2014.06.063
8. Chen, J., Ji, Q., Zheng, P., Chen, T., Wang, C., 2010. Floatation and control of granular sludge in a high-rate anammox reactor. Water Res. 44, 3321–3328. https://doi.org/10.1016/j.watres.2010.03.016
9. Chen, L., Chen, H., Lu, D., Xu, X., Zhu, L., 2020. Response of methanogens in calcified anaerobic granular sludge: Effect of different calcium levels. J. Hazard. Mater. 122131. https://doi.org/10.1016/j.jhazmat.2020.122131
10. Dapena-mora, A., Campos, J.L., Mosquera-corral, A., Mendez, R., 2004. Stability of the ANAMMOX process in a gas-lift reactor and a SBR. J. Biotechnol. 110, 159–170. https://doi.org/10.1016/j.jbiotec.2004.02.005
11. Graaf, A.A. Van De, Bruijn, P. De, Robertson, L.A., Jetten, M.M., Kuenen, J.G., 1996. Autotrophic growth of anaerobicammonium-oxidizing micro-organisms in a fluidized bed reactor. Microbiology 142, 2187–2196.
12. Guo, Y., Li, Y., 2020. Hydroxyapatite crystallization-based phosphorus recovery coupling with the nitrogen removal through partial nitritation/anammox in a single reactor. Water Res. 187. https://doi.org/10.1016/j.watres.2020.116444
13. Gustafsson, J.P., 2014. Visual MINTEQ 3 . 1 user guide 1–73.
14. Heijnen, J.J., Loosdrecht, M.C.M. Van, Tijhuis, L., 1992. A Black Box Mathematical Model to Calculate Auto- and Heterot rophic Biomass Yields Based on Gibbs Energy Dissipation, in: Biotechnology and Bioengineering, Vol. 40. pp. 1139–1154.

15. Hu, Q., Kang, D., Wang, R., Ding, A., Abbas, G., Zhang, M., 2018. Characterization of oligotrophic AnAOB culture : morphological , physiological , and ecological features. Environ. Biotechnol. 995–1003. https://doi.org/https://doi.org/10.1007/s00253-017-8587-8

16. Johansson, S., Ruscalleda, M., Colprim, J., 2017. Phosphorus recovery through biologically induced precipitation by partial nitritation-anammox granular biomass. Chem. Eng. J. 327, 881–888. https://doi.org/10.1016/j.cej.2017.06.129

17. Kang, D., Guo, L., Hu, Q., Xu, D., Yu, T., Li, Y., Zeng, Z., Li, W., 2019. Surface convexity of anammox granular sludge : Digital characterization , state indication and formation mechanism. Environ. Int. 131, 105017. https://doi.org/10.1016/j.envint.2019.105017

18. Langelier, W.F., 1936. THE ANALYTICAL CONTROL OF ANTI-CORROSION WATER TREATMENT Author(s): Am. Water Work Assoc. 28, 1500–1521.

19. Langerak, E.P.A.V.A.N., Ramaekers, H., Wiechers, J., Hamelers, H.V.M., Lettinga, G., 2000. IMPACT OF LOCATION OF CaCO 3 PRECIPITATION ON THE DEVELOPMENT OF INTACT ANAEROBIC SLUDGE. Water Res. 34, 437–446.

20. Langerak, E.P.A. Van, Hamelers, H.V.M., Lettinga, G., 1997. INFLUENT CALCIUM REMOVAL BY CRYSTALLIZATION REUSING ANAEROBIC EFFLUENT ALKALINITY. Water Sci. Technol. 36, 341–348. https://doi.org/10.1016/S0273-1223(97)00541-6

21. Li, W., Zheng, P., Ji, J., Zhang, M., Guo, J., Zhang, J., Abbas, G., 2014. Floatation of granular sludge and its mechanism : A key approach for high-rate denitrifying reactor. Bioresour. Technol. J. 152, 414–419.

https://doi.org/10.1016/j.biortech.2013.11.056
22. Lin, X., Wang, Y., 2017. Microstructure of anammox granules and mechanisms endowing their intensity revealed by microscopic inspection and rheometry. Water Res. https://doi.org/10.1016/j.watres.2017.04.053
23. Lin, Y.M., Lotti, T., Sharma, P.K., Loosdrecht, M.C.M. Van, 2013. Apatite accumulation enhances the mechanical property of anammox granules. Water Res. 47, 4556–4566. https://doi.org/10.1016/j.watres.2013.04.061
24. Lotti, T., Kleerebezem, R., Lubello, C., Loosdrecht, M.C.M. Van, 2014. Physiological and kinetic characterization of a suspended cell anammox culture. Water Res. 60, 1–14. https://doi.org/10.1016/j.watres.2014.04.017
25. Lotti, T., Star, W.R.L. Van Der, Kleerebezem, R., Lubello, C., Loosdrecht, M.C.M. Van, van der Star, W.R.L., Kleerebezem, R., Lubello, C., van Loosdrecht, M.C.M., 2012. The effect of nitrite inhibition on the anammox process. Water Res. 46, 2559–2569. https://doi.org/http://dx.doi.org/10.1016/j.watres.2012.02.011
26. Ma, H., Xue, Y., Zhang, Y., Kobayashi, T., Kubota, K., Li, Y., 2020. Simultaneous nitrogen removal and phosphorus recovery using an anammox expanded reactor operated at 25 °C. Water Res. 115510. https://doi.org/10.1016/j.watres.2020.115510
27. Mazzoli, L., Munz, G., Lotti, T., Ramazzotti, M., 2020. A novel universal primer pair for prokaryotes with improved performances for anammox containing communities. Sci. Rep. 1–7. https://doi.org/https://doi.org/10.1038/s41598-020-72577-4
28. Niccolai, E., Russo, E., Baldi, S., Ricci, F., Nannini, G., Pedone, M., Stingo, F.C., Taddei, A., Ringressi, M.N., Bechi, P., Mengoni, A., Fani, R., Bacci, G.,

Fagorzi, C., Chiellini, C., Prisco, D., Ramazzotti, M., Amedei, A., 2020. Significant and conflicting correlation of IL-9 with Prevotella and Bacteroides in human 2 colorectal cancer. prepint version. https://doi.org/https://doi.org/10.1101/2020.04.28.066001

29. Niftrik, L. Van, Geerts, W.J.C., Donselaar, E.G. Van, Humbel, B.M., Webb, R.I., Fuerst, J.A., Verkleij, A.J., Jetten, M.S.M., Strous, M., 2008. Linking Ultrastructure and Function in Four Genera of Anaerobic Ammonium-Oxidizing Bacteria : Cell Plan , Glycogen Storage , and Localization of Cytochrome c Proteins □. J. Bacteriol. 190, 708–717. https://doi.org/10.1128/JB.01449-07
30. Oshiki, M., Satoh, H., Okabe, S., 2016. Minireview Ecology and physiology of anaerobic ammonium oxidizing bacteria. Environ. Microbiol. https://doi.org/10.1111/1462-2920.13134
31. Takahashi, S., Tomita, J., Nishioka, K., Hisada, T., Nishijima, M., 2014. Development of a Prokaryotic Universal Primer for Simultaneous Analysis of Bacteria and Archaea Using Next-Generation Sequencing. PLoS One 9. https://doi.org/10.1371/journal.pone.0105592
32. Tijhuis, L., Loosdrecht, M.C.M. Van, 1994. Solids Retention Time in Spherical Biofilms in a Biofilm Airlift Suspension Reactor 44, 867–879.
33. Trigo, C., Campos, J.L., Garrido, J.M., Mendez, R., 2006. Start-up of the Anammox process in a membrane bioreactor. J. Biotechnol. 126, 475–487. https://doi.org/10.1016/j.jbiotec.2006.05.008
34. Wu, S., Zou, S., Liang, G., Qian, G., He, Z., 2018. Enhancing recovery of magnesium as struvite from land fi ll leachate by pretreatment of calcium with simultaneous reduction of liquid volume via forward osmosis. Sci. Total Environ. 610–611, 137–146. https://doi.org/10.1016/j.scitotenv.2017.08.038

35. Xue, Y., Ma, H., Kong, Z., Guo, Y., Li, Y., 2020. Bulking and floatation of the anammox-HAP granule caused by low phosphate concentration in the anammox reactor of expanded granular sludge bed (EGSB). Bioresour. Technol. 310, 123421. https://doi.org/10.1016/j.biortech.2020.123421

36. Xue, Y., Ma, H., Kong, Z., Li, Y., 2021. Formation Mechanism of hydroxyapatite encapsulation in Anammox-HAP Coupled Granular Sludge 193. https://doi.org/10.1016/j.watres.2021.116861

37. Zhang, W., Wang, D., Jin, Y., 2017. Effects of inorganic carbon on the nitrous oxide emissions and microbial diversity of an anaerobic ammonia oxidation reactor. Bioresour. Technol. https://doi.org/10.1016/j.biortech.2017.11.027

Figure Captions

Figure 1 Experimental set-up. Water line (blue), gas line (dashed red) and sensors (dotted green). Influent port (1); gas recirculation inlet (2); water-lock and overpressure control (3); moisture trap (4); vacuum pump (5); thermostatic unit (6).

Figure 2 Influent and effluent nitrogen concentration (a); NLR and NO_2^- removal efficiency (b). Nitrate was dosed in phase 1 only, at influent concentration of 150 mgN-NO_3^-/l.

Figure 3 VSS concentration in the reactor and VSS/TSS ratio. Dotted vertical lines define the hard-water feeding period.

Figure 4 Results on activity tests versus the applied SNLR. MSAA from manometric assays (black columns) and from in-situ batch tests (white column); SNLR (--o--).

Figure 5 Microbial diversity profiles over the experimental work, at class (a) and genus level (b). Only Operational Taxonomic Units with relative abundance higher than 1% are displayed.

Figure 6 Pictures of anammox granular biomass on day 155: on a 0.5-mm sieve on the left and after incineration at 550° on the right (a). SEM images of a granules showing evident mineral precipitation exhibiting two types of surfaces: a biofilm-like uniform layer over a rough irregular surface with crystal precipitates (b). TEM observations on sections of granules not affected by mineral precipitation on the left and with evident precipitation on the right (c).

Tables and figures

Table 1 Tap water and mineral medium characterization for alkalinity, total phosphorous and hardness related components.

Parameter	Tap water	Influent on days 36-50 (distilled water and nutrient addition)	Influent on days 60-120 (tap water and nutrient addition)
Ca^{2+} [mg/l]	133±18	54	187
Mg^{2+} [mg/l]	45.5±6	10	55.4
Na^{+} [mg/l]	129±18	849	970-1422
K^{+} [mg/l]	2.41±0.38	7.1	9.6
$C\text{-}HCO_3^-$		440	495-730
Total P [mgP/l]	0.067±0.003	5	5

Table 2 Applied conditions during the experimental phases.

Experimental phases	Days	HRT [d]	NLR [gN-NO_2^-/l/d]
P1-start up	1-15	1.1±0.3	0.02-0.09
P2- NLR increase	15-130	1.1 to 1.6	0.09-0.50
P3 – Process disruption	131-154	1.6±0.2	0.50±0.05
Off-site biomass rescue	155-177	-	-
P4- Process restoration	178-270	1.6±0.2	0.22±0.02

Table 3 Observed stoichiometry during the operational phases

Phase	**Days**	**NO_2^-/ NH_4^+ [gN/gN]**	**NO_3^-/ NH_4^+ [gN/gN]**
P1-start up	1-15	-	-
P2- NLR increase	15-130	1.146 ±0.080	0.167±0.063
P3 – Process disruption	131-155	1.271±0.045	0.165±0.008
Off-site biomass rescue	155-177	-	-
P4- Process restoration	178-225	1.322± 0.092	0.211±0.072
	226-270	1.182± 0.091	0.164±0.058

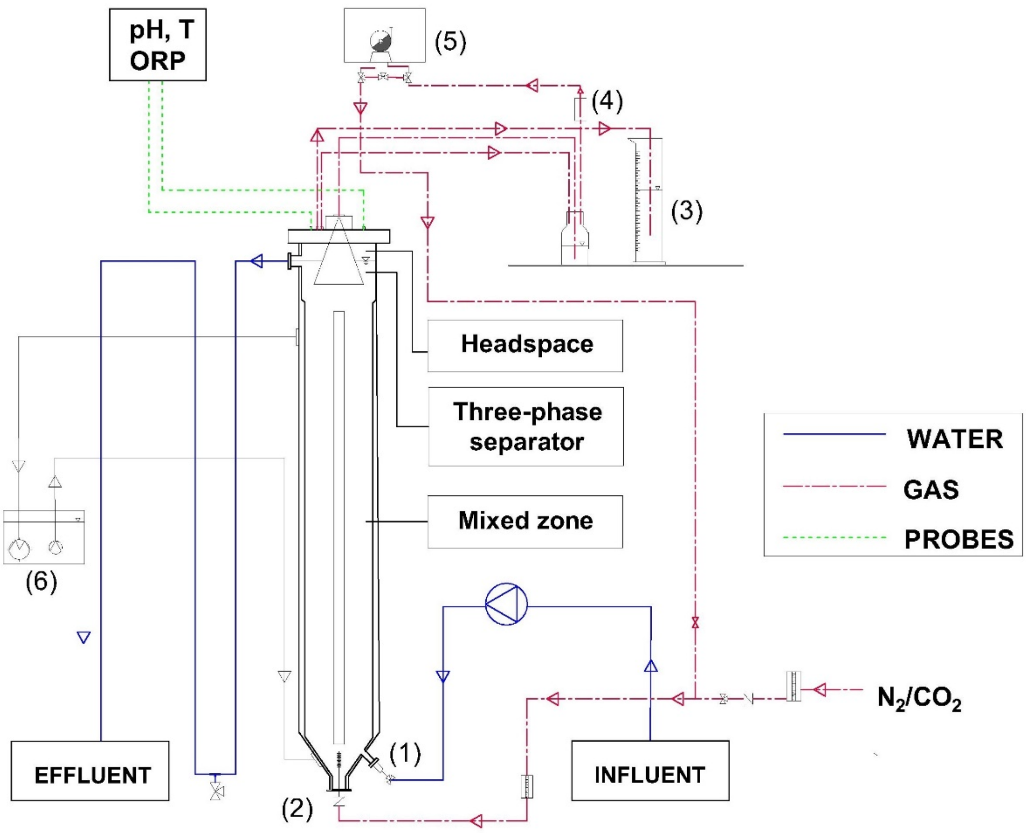

Figure 1 Experimental set-up. Water line (blue), gas line (dashed red) and sensors (dotted green). Influent port (1); gas recirculation inlet (2); water-lock and overpressure control (3); moisture trap (4); vacuum pump (5); thermostatic unit (6).

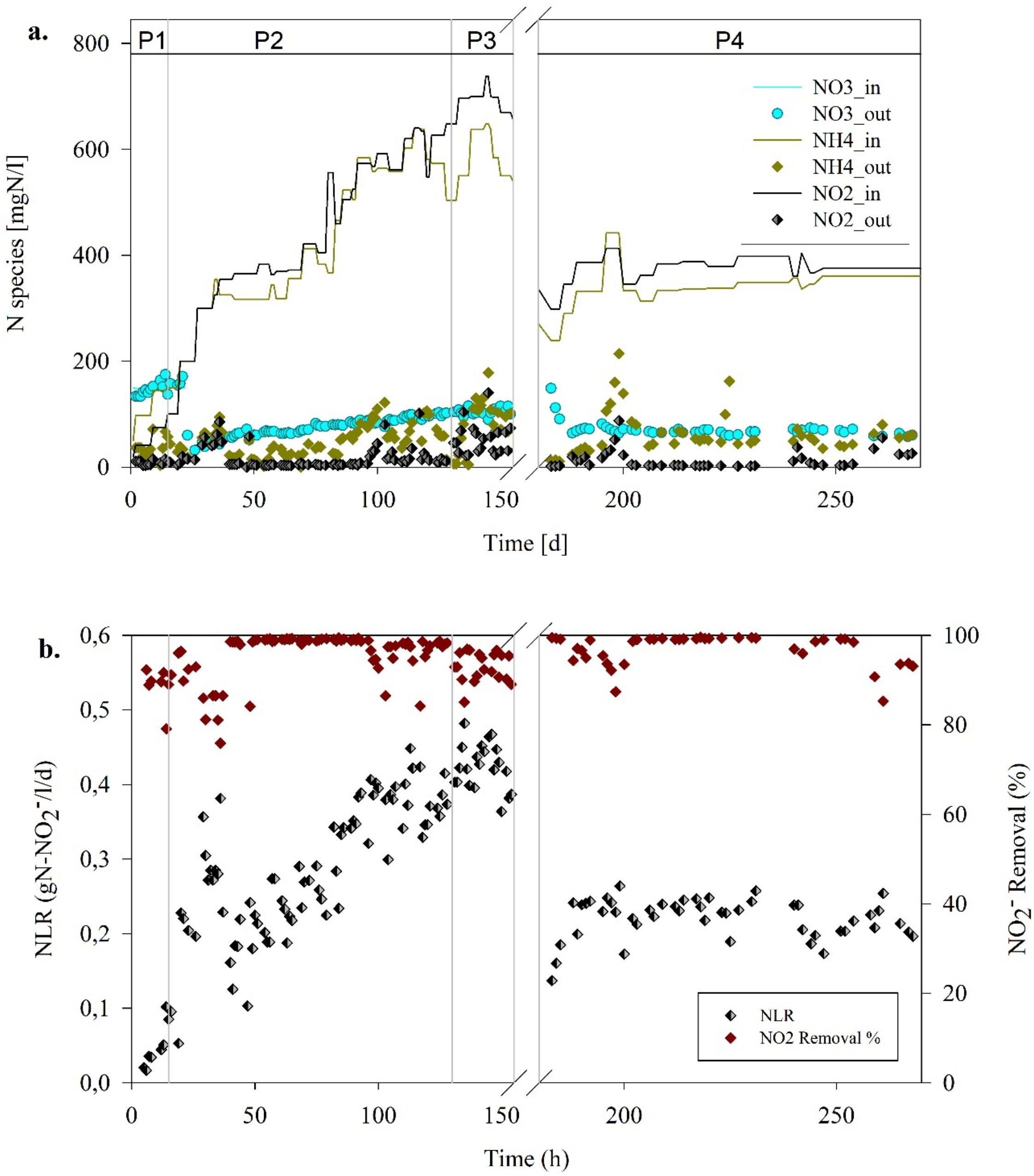

654

655 **Figure 2 Influent and effluent nitrogen concentration (a); NLR and NO_2^- removal**

656 **efficiency (b). Nitrate was dosed in phase 1 only, at influent concentration of 150**

657 **mgN-NO_3^-/l.**

658

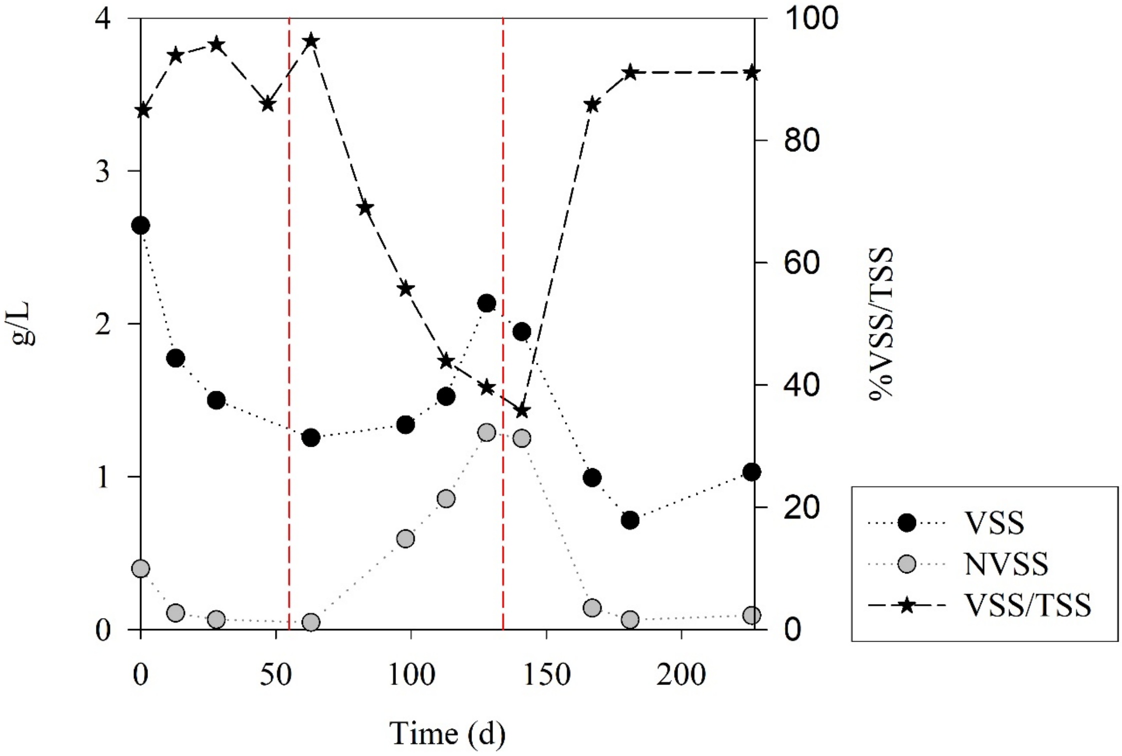

Figure 3 VSS concentration in the reactor and VSS/TSS ratio. Dotted vertical lines define the hard-water feeding period.

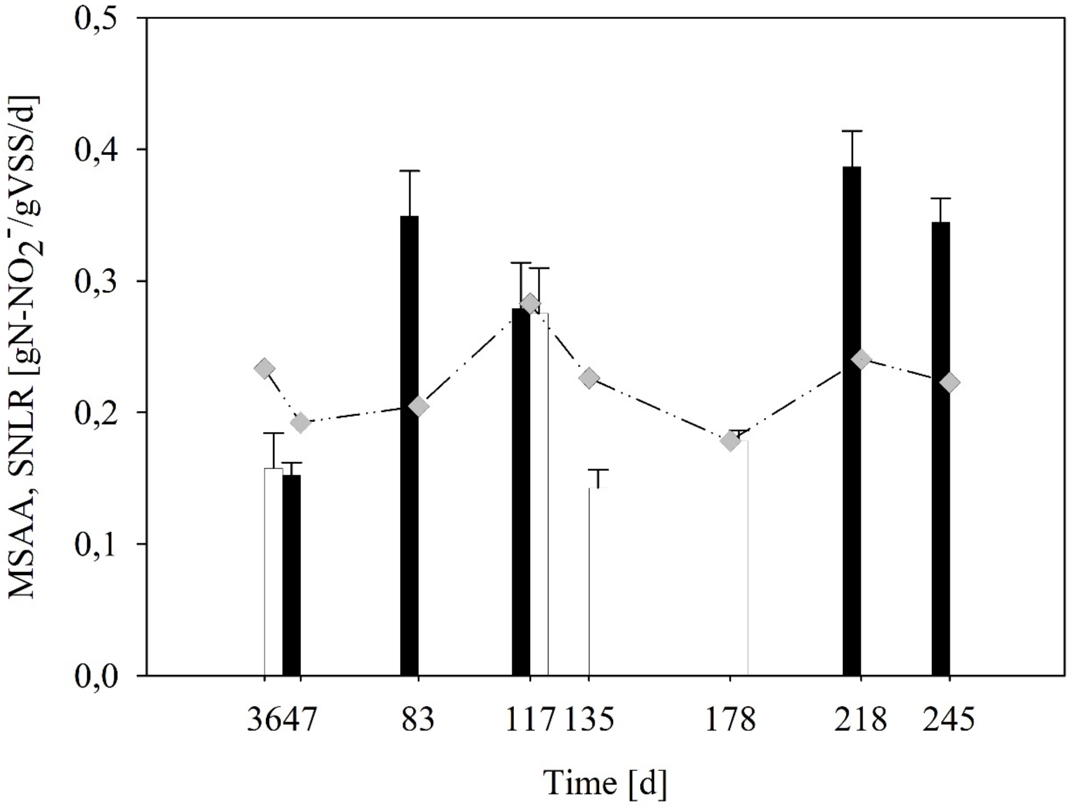

Figure 4 Results on activity tests versus the applied SNLR. MSAA from manometric assays (black columns) and from in-situ batch tests (white column); SNLR (--o--).

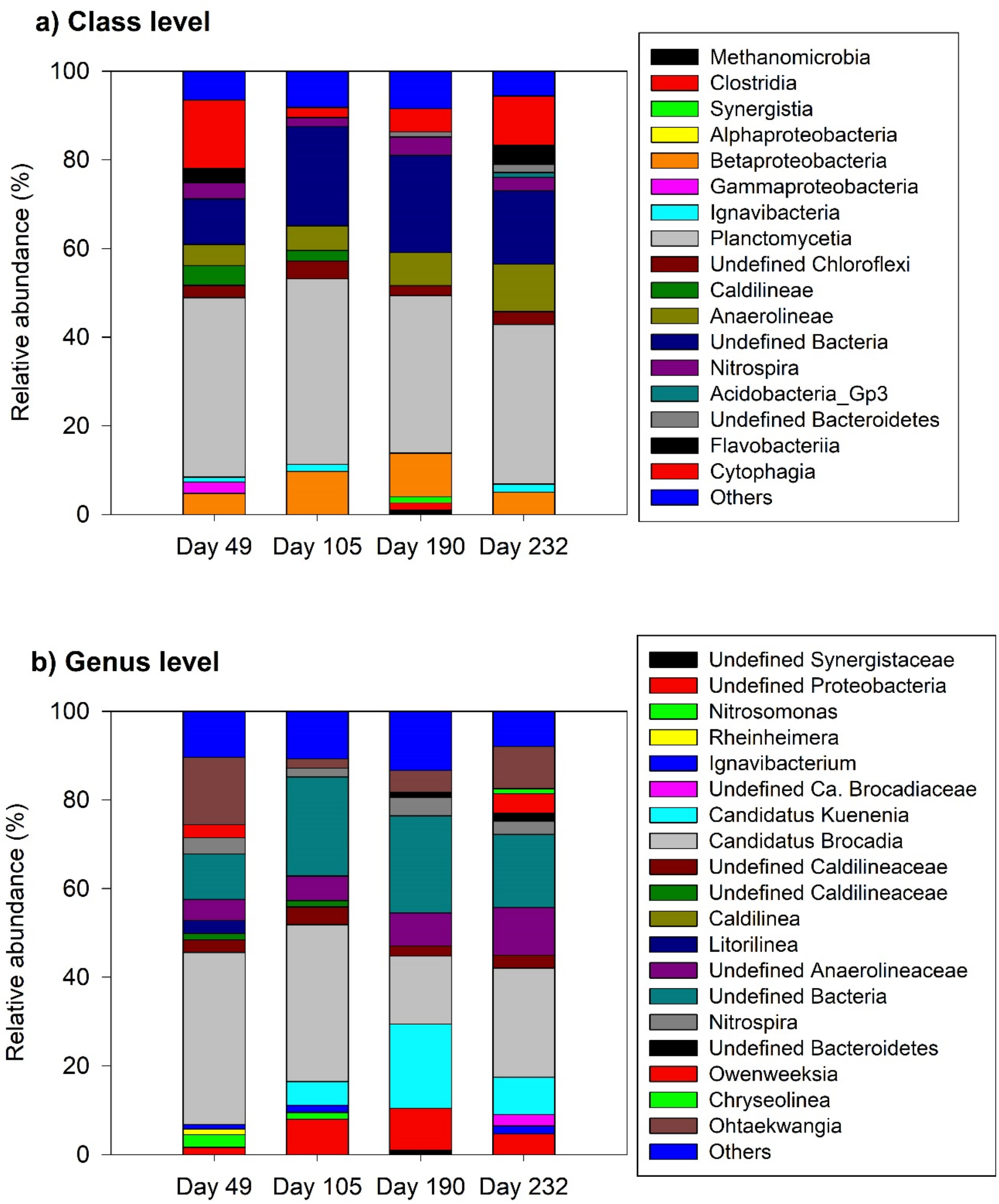

Figure 5 Microbial diversity profiles over the experimental work, at class (a) and genus level (b). Only Operational Taxonomic Units with relative abundance higher than 1% are displayed.

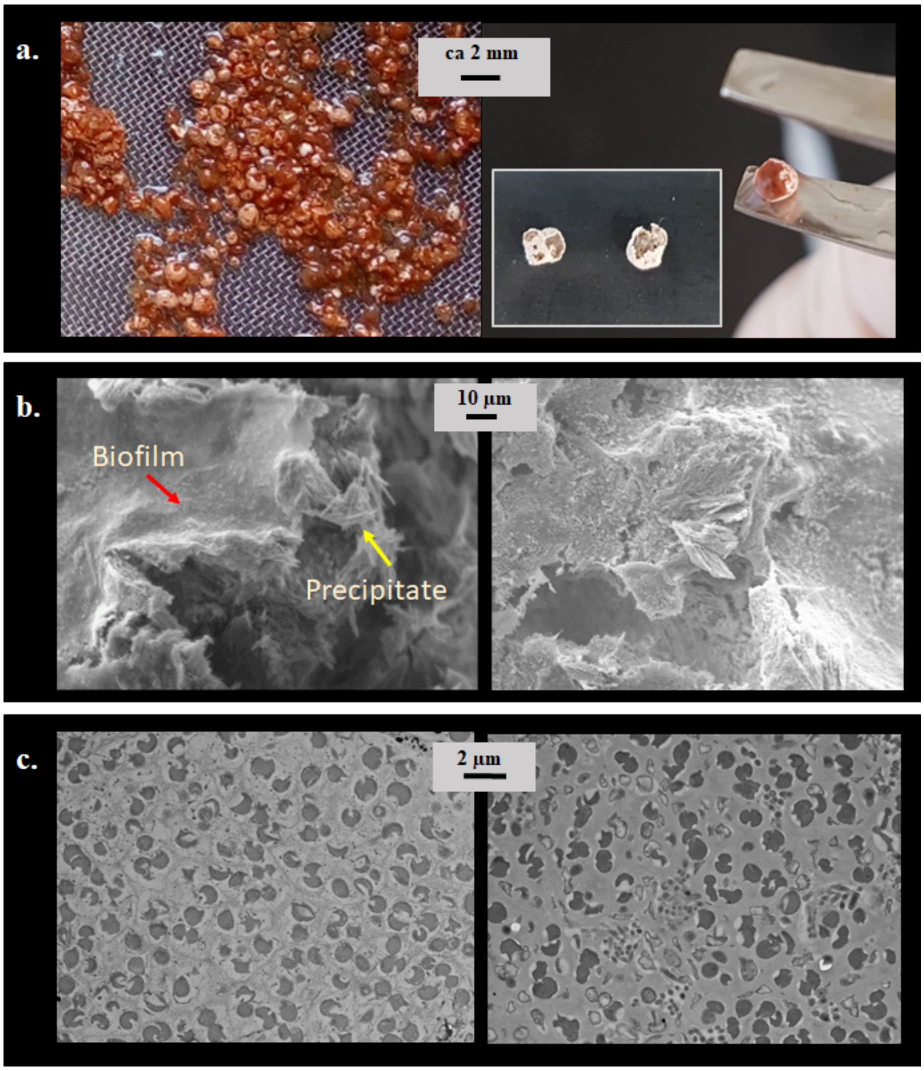

Figure 6 Pictures of anammox granular biomass on day 155: on a 0.5-mm sieve on the left and after incineration at 550° on the right (a). SEM images of a granules showing evident mineral precipitation exhibiting two types of surfaces: a biofilm-like uniform layer over a rough irregular surface with crystal precipitates (b). TEM observations on sections of granules not affected by mineral precipitation on the left and with evident precipitation on the right (c).